ARMY RESEARCH LABORATORY

Nondestructive Early Detection of Metal Corrosion in Pigmented Coatings with Fluorescent Smart Materials (First-year Report)

by Joshua A. Orlicki, André A. Williams, Joseph Labukas, John A. Escarsega, and Brian Placzankis

ARL-MR-0820 **May 2012**

NOTICES

Disclaimers

The findings in this report are not to be construed as an official Department of the Army position unless so designated by other authorized documents.

Citation of manufacturer's or trade names does not constitute an official endorsement or approval of the use thereof.

Destroy this report when it is no longer needed. Do not return it to the originator.

Army Research Laboratory
Aberdeen Proving Ground, MD 21005

ARL-MR-0820 **May 2012**

Nondestructive Early Detection of Metal Corrosion in Pigmented Coatings with Fluorescent Smart Materials (First-year Report)

Joshua A. Orlicki, André A. Williams, Joseph Labukas, John A. Escarsega, and Brian Placzankis
Weapons and Materials Research Directorate, ARL

REPORT DOCUMENTATION PAGE

Form Approved
OMB No. 0704-0188

1. REPORT DATE *(DD-MM-YYYY)*	2. REPORT TYPE	3. DATES COVERED (From - To)
May 2012	DRI	October 1, 2010 to September 30, 2011

4. TITLE AND SUBTITLE
Nondestructive Early Detection of Metal Corrosion in Pigmented Coatings with Fluorescent Smart Materials (First-year Report)

5a. CONTRACT NUMBER

5b. GRANT NUMBER

5c. PROGRAM ELEMENT NUMBER

6. AUTHOR(S)
Joshua A. Orlicki, André A. Williams, Joseph Labukas, John E. Escarsega, and Brian Placzankis

5d. PROJECT NUMBER

5e. TASK NUMBER

5f. WORK UNIT NUMBER

7. PERFORMING ORGANIZATION NAME(S) AND ADDRESS(ES)
U.S. Army Research Laboratory
ATTN: RDRL-WMM-G
Aberdeen Proving Ground, MD 21005

8. PERFORMING ORGANIZATION REPORT NUMBER
ARL-MR-0820

9. SPONSORING/MONITORING AGENCY NAME(S) AND ADDRESS(ES)

10. SPONSOR/MONITOR'S ACRONYM(S)

11. SPONSOR/MONITOR'S REPORT NUMBER(S)

12. DISTRIBUTION/AVAILABILITY STATEMENT
Approved for public release; distribution unlimited.

13. SUPPLEMENTARY NOTES

14. ABSTRACT
Fluorescent dyes were studied in an effort to develop molecules suitable to signal the onset of metal corrosion under a paint or coating. Rhodamine B and fluorescein were chemically modified to determine the effect of steric hindrance and electron withdrawing/donating substituents on the selective binding of these dyes to various metals. Rhodamine B and fluorescein were converted into the corresponding hydrazide to provide a precursor material. The hydrazides were then reacted with various diphenyl and dialkyl ketones to determine the impact of bulky groups on dye-metal binding. Electronic effects were probed as the hydrazide precursors were reacted with various aldehydes that contained substituted phenyl rings. Fluorescence measurements were used to determine the impact of each substitution on dye-metal binding efficiency and selectivity.

15. SUBJECT TERMS
Corrosion detection, fluorescence, CARC, fluorescein, rhodamine

16. SECURITY CLASSIFICATION OF:			17. LIMITATION OF ABSTRACT	18. NUMBER OF PAGES	19a. NAME OF RESPONSIBLE PERSON
a. REPORT	b. ABSTRACT	c. THIS PAGE			Joshua A. Orlicki
Unclassified	Unclassified	Unclassified	UU	24	19b. TELEPHONE NUMBER (*Include area code*) (410) 306-0931

Contents

List of Figures

List of Tables

1. Objective

Corrosion of metal causes deterioration of Department of Defense (DoD) facilities, vehicles, and weapons and costs the Government $9–20 billion per year (*1*). Corrosion can go undetected underneath pigmented coatings and the development of additives that enable nondestructive detection of the early stages of corrosion could significantly benefit the Army's battlefield readiness. Early detection would reduce lifetime acquisition costs and maintain assets in optimal condition by triggering early maintenance of the underlying metal surface before substantial damage could occur. Therefore, development of nondestructive methods for detecting the early onset of metal corrosion on military assets is important.

2. Approach

Recently, fluorescent probes were developed for the sensing and reporting of cationic transition-metal ions. Most notably, rhodamine B and fluorescein dyes were used as fluorescent probes in the detection of Cu^{2+}, Pb^{2+}, Zn^{2+}, Hg^{2+}, and Fe^{3+} (*2*–*9*). These dyes were ideal for sensing applications because of the vastly different fluorescent properties exhibited from the nonfluorescent spirolactam ring-closed form ("off" signal) and the fluorescent ring-open form ("on" signal). These probes were nonfluorescent and were undetectable under ultraviolet (UV) light but became fluorescent upon binding to the appropriate metal cation. Augustyniak et al. (*2*) reported that a rhodamine B based dye, spiro[1H-isoindole-1,9'-[9H]xanthen]-3(2H)-one, 3',6'-bis(diethylamino)-2-[(1-methylethylidene)amino] (FDI), was a selective chemosensor for Fe^{3+} (figure 1).

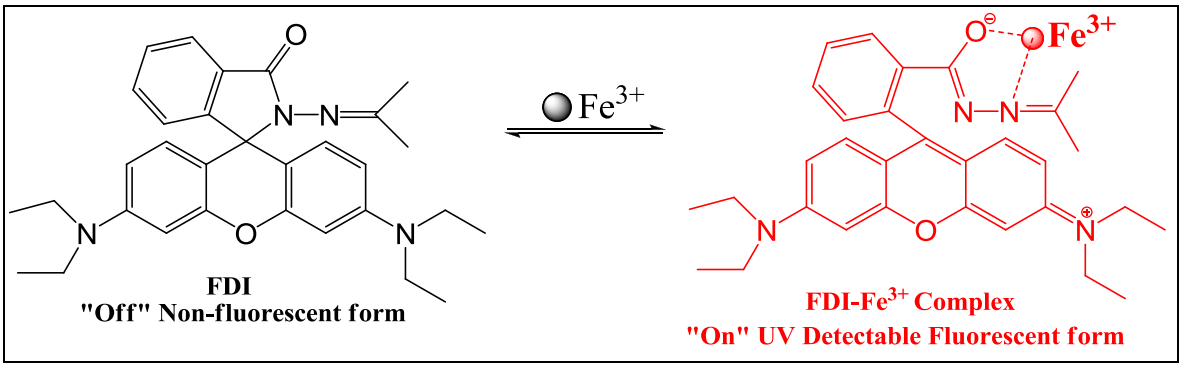

Figure 1. Turn on fluorescence of FDI.

The objective of this project was to develop corrosion-sensing indicators that can be incorporated into epoxy and urethane coatings to enable the nondestructive detection of early stage metal corrosion. Detection of corrosion would be accomplished by simple illumination of the coated

surface with UV light. These fluorescent corrosion-sensing indicators would ideally only interact with metal ions generated during the corrosion process (figure 1). In practice, several cations may form fluorescently active complexes. In an effort to control the binding and fluorescence activity of these dyes, rhodamine B and fluorescein were chemically modified to study the effect of steric hindrance and electron density on the selective binding of these dyes to various metals. Rhodamine B and fluorescein hydrazides were reacted with various diphenyl and dialkyl ketones to determine the impact of bulky groups on dye-metal binding. Electronic effects were probed as the hydrazide precursors were reacted with various aldehydes that contained substituted phenyl rings. Fluorescence and UV/visible (Vis) measurements were conducted to determine the impact of sterics and electronics on dye-metal binding efficiency and selectivity.

3. Results

The rhodamine B and fluorescein hydrazone dyes were synthesized in two steps. In the first step, rhodamine B and fluorescein were converted into the corresponding hydrazide to provide a precursor hydrazide material. In the second step, the hydrazides were reacted with various ketones and aldehydes to form a wide variety of hydrazone dyes (tables 1 and 2).

Table 1. Rhodamine B dyes.

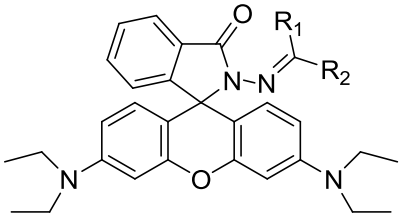

Rhodamine B Hydrazone Dye

Dyes	Synthesized Compounds	
	R_1	R_2
1	CH_3	CH_3
2	CH_2CH_2	$CH_2CH_2CH_2$
3	H	C_6H_5
4	H	C_6H_4-4-NO_2

Table 2. Fluorescein dyes.

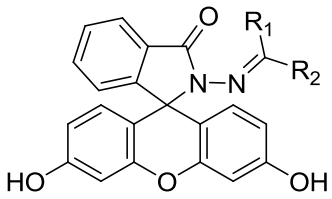

Fluorescein Hydrazone Dye

Dyes	Synthesized Compounds	
	R_1	R_2
5	CH_3	CH_3
6	H	C_6H_5
7	H	C_6H_4-4-NO_2
8	H	C_6H_4-4-$N(CH_3)_2$

3.1 Synthesis of Rhodamine B hydrazides

Rhodamine B (10.0 g, 20.9 mmol) was stirred in ethanol (EtOH) at room temperature (rt). Hydrazine (30.0 mL, 956 mmol) was added to the mixture, which was then refluxed at 80–85 °C for 4 h. The reaction mixture was cooled to rt, and then the solvent was removed with a rotary evaporator. The resulting brown/black solid was dissolved in 1 M hydrochloric acid (HCl) (typically 200 mL) at rt, and then 1 M sodium hydroxide (NaOH) (typically 700 mL) was added to the red solution until the solution reached a pH of 10. As the pH of the solution approached 7, precipitation occurred as the ammonium salt was deprotonated, which resulted in a pink suspension that persisted at elevated pH levels. The pink mixture was allowed to stir for 1 h, and then isolated using gravity filtration. The pink solid was washed repeatedly with water, and then left to air dry overnight (figure 2).

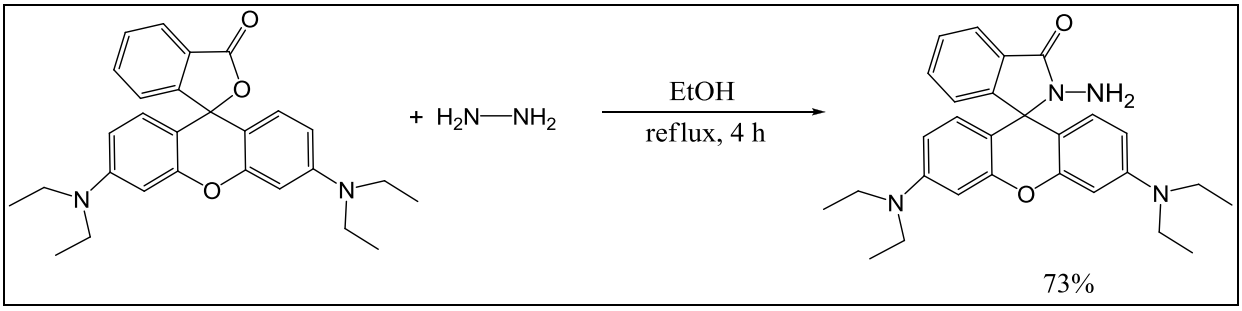

Figure 2. Scheme 1: Synthesis of rhodamine B hydrazide.

3.2 Synthesis of Fluorescein Hydrazide

Fluorescein (7.00 g, 21.1 mmol) was stirred in EtOH at rt. Hydrazine (8.40 mL, 315 mmol) was added to the mixture, and then the bright orange mixture was heated at reflux for 4 h. The reaction mixture was cooled to rt and then solvent was removed with a rotary evaporator. The

resulting orange oil or solid was placed under vacuum overnight. The oil/solid was dissolved in methanol (MeOH), and any insoluble material was removed via gravity filtration. A yellow solid was precipitated out of solution with water. The resulting mixture was allowed to stand overnight. The yellow solid was isolated via gravity filtration and then dried overnight in a vacuum oven at 60 °C (figure 3).

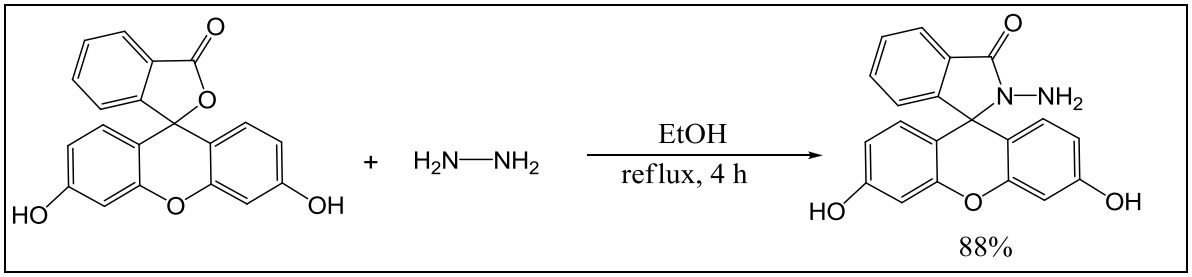

Figure 3. Scheme 2: Synthesis of fluorescein hydrazide.

3.3 General Procedure for the Synthesis of Hydrazones

Rhodamine or fluorescein hydrazide (2.02 mmol) was stirred in 25 mL of EtOH at rt. The appropriate benzaldehye/ketone (8.08 mmol) was added, and then the reaction was heated at reflux for 24 h. Three drops of acetic acid was used as an acid catalyst for reactions that used ketones. The reaction was cooled to rt and then the solvent was removed with a rotary evaporator (figure 4). Rhodamine B hydrazone dyes were triturated in hexane or water, while fluorescein dyes were triturated in dichloromethane (DCM). Rhodamine B and fluorescein hydrazone dyes were then recrystallized in MeOH/water.

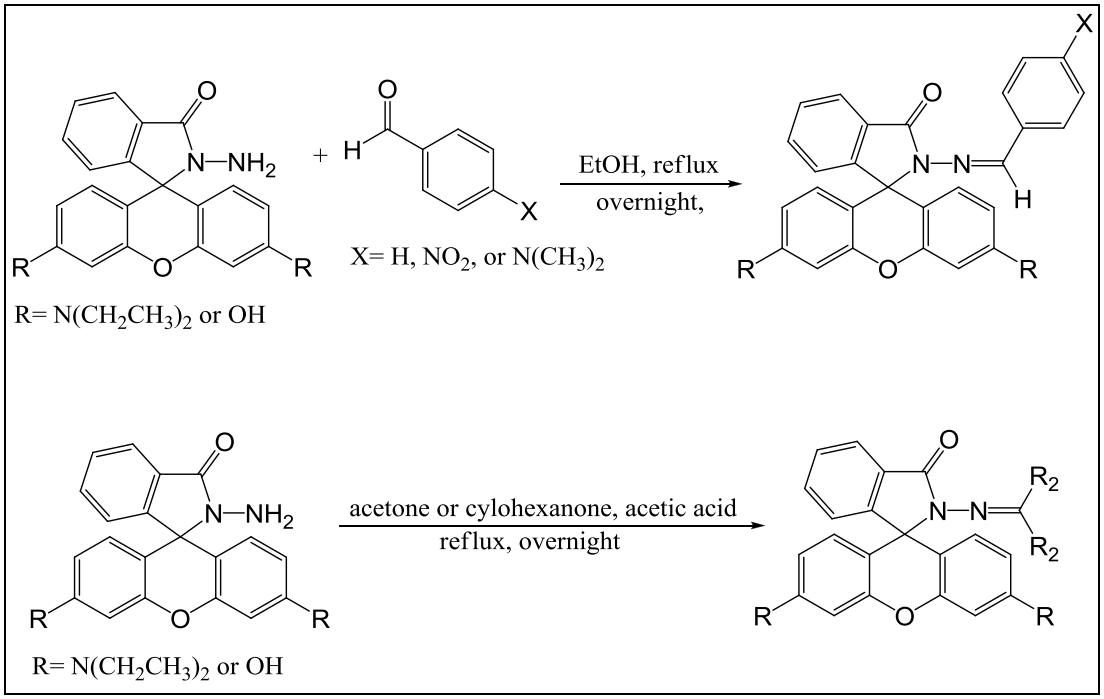

Figure 4. Scheme 3: General synthesis of hydrazone dyes.

^{1}H and ^{13}C nuclear magnetic resonance (NMR) were performed on the synthesized hydrazone dyes. The following section is the summary of peaks and chemical shifts associated with the molecules as described in tables 1 and 2:

- **Compound 1.** % yield: 48%. ^{1}H NMR (deuterated chloroform [$CDCl_3$]), δ ppm: 1.13 (m, 12H), 1.79 (s, 3H), 1.94 (s, 3H), 3.31 (m, 8H), 6.26-6.52 (m, 6H), 7.10 (m, 1H), 7.43 (m, 2H), 7.88 (m, 1H). ^{13}C NMR ($CDCl_3$), δ ppm: 12.3, 13.13, 13.97, 14.80, 21.06, 21.91, 22.77, 23.61, 25.18, 26.03, 26.88, 27.72, 44.32, 45.22, 46.11, 67.02, 98.21, 99.25, 105.5, 107.3, 108.4, 109.2, 123.2, 124.2, 125.3, 128.5, 128.9, 129.5, 130.0, 130.9, 131.7, 132.5, 133.6, 149.5, 152.7, 154.4, 161.5, 167.1, 175.2.
- **Compound 2.** % yield: 87%. ^{1}H NMR ($CDCl_3$), δ ppm: 1.15 (t, 12H), 1.25 (m, 2H), 1.46 (m, 2H), 1.54 (m, 2H), 1.64 (bm, 3H), 2.15 (t, 2H), 2.30 (t, 2H), 3.31 (s, 8H), 6.27 (dd, 1H), 6.28 (dd, 1H), 6.39 (dd, 2H), 6.50 (s, 1H), 6.52 (s, 1H), 7.16 (m, 1H), 7.45 (m, 2H), 7.90 (m, 1H). m.p. 168.4–169.6 °C. ^{13}C NMR ($CDCl_3$), δ ppm: 12.25, 13.08, 13.92, 14.75, 25.60, 26.43, 27.38, 28.46, 29.32, 31.54, 32.40, 33.25, 35.78, 36.63, 37.49, 44.38, 45.28, 46.17, 66.96, 98.28, 99.33, 105.4, 107.3, 108.2, 109.3, 123.3, 124.2, 124.4, 125.3, 128.5, 128.8, 129.6, 129.8, 132.2, 133.42, 149.5, 151.9, 154.8, 160.9, 167.1.
- **Compound 3.** % yield: 72%. ^{1}H NMR ($CDCl_3$), δ ppm: 1.15 (t, 12H), 3.31 (s, 8H), 6.23 (m, 2H), 6.43 (m, 2H), 6.51 (t, 2H), 7.11 (m, 1H), 7.25 (m, 3H), 7.46 (m, 2H), 7.54 (m, 2H), 7.98 (m, 1H), 8.67 (m, 1H). ^{13}C NMR ($CDCl_3$), δ ppm:12.26, 13.10, 13.93, 14.77, 44.33, 45.22, 46.12, 66.88, 98.24, 99.28, 106.9, 108.4, 109.5, 123.7, 124.2, 124.8, 125.3, 127.9, 128.4, 128.6, 129.0, 129.5, 129.7, 130.2, 133.8, 134.8, 136.3, 147.5, 148.6, 149.8, 152.8, 154.0. m.p. 229.4–230.2 °C.
- **Compound 4.** % yield: 82%. ^{1}H NMR ($CDCl_3$), δ ppm: 1.16 (t, 12H), 3.31 (dd, 8H), 6.25 (dd, 2H), 6.45-6.50 (m, 4H), 7.15 (dd, 1H), 7.5-7.54 (m, 2H), 7.65 (dd, 2H), 7.99 (dd, 1H), 8.10 (dd, 2H), 8.86 (s, 1H). ^{13}C NMR ($CDCl_3$), δ ppm: 12.22, 13.06, 13.89, 14.72, 44.33, 45.23, 46.11, 67.31, 98.17, 99.22, 106.7, 108.4, 109.4, 124.0, 124.5, 125.1, 125.6, 128.2, 128.4, 128.9, 129.3, 129.4, 130.1, 134.2, 135.3, 142.5, 144.4, 145.5, 148.9, 149.9, 152.2, 154.2, 166.0. m.p. 237.2–237.9 °C.
- **Compound 5.** % yield: 77%. ^{1}H NMR (*d*-dimethylsulfoxide [DMSO]), δ ppm: 1.73 (s, 3H), 1.82 (s, 3H), 6.44 (m, 4H), 6.52 (m, 2H), 7.02 (m, 1H), 7.51 (m, 2H), 7.78 (m, 1H). ^{13}C NMR (*d*-DMSO), δ ppm: 21.28, 22.14, 22.99, 23.84, 25.01, 25.85, 26.70, 27.55, 30.77, 31.61, 32.45, 33.29, 66.23, 103.0, 104.1, 111.4, 112.9, 114.0, 123.5, 124.4, 124.6, 125.5, 129.4, 130.4, 130.6, 131.0, 133.6, 134.7, 152.7, 153.5, 159.6, 161.3, 174.8.

- **Compound 6.** % yield: 72%. ^{1}H NMR (*d*-DMSO), δ ppm: 6.42 (m, 2H), 6.45 (m, 2H), 6.62 (s, 2H), 7.10 (dd, 1H), 7.32 (s, 3H), 7.38 (m, 2H), 7.56 (t, 1H), 7.61 (t, 1H), 7.89 (dd, 1H), 8.98 (s, 1H). m.p. 269.6-270.9 °C. ^{13}C NMR (*d*-DMSO), δ ppm: 66.69, 103.3, 104.3, 111.5, 113.1, 114.2, 124.0, 124.6, 125.1, 125.7, 127.6, 128.6, 128.9, 129.6, 129.9, 130.4, 130.7, 131.0, 134.8, 135.8, 150.9, 151.1, 151.7, 153.6, 160.0, 165.
- **Compound 7.** % yield: 56%. ^{1}H NMR (*d*-DMSO), δ ppm: 6.44 (m, 2H), 6.48 (m, 2H), 6.65 (s, 2H), 7.14 (dd, 1H), 7.59 (t, 1H), 7.65 (dd, 3H), 7.93 (dd, 1H), 8.18 (dd, 2H), 9.11 (s, 1H). ^{13}C NMR (*d*-DMSO), δ ppm: 66.9, 103.4, 104.4, 111.2, 113.2, 114.3, 124.3, 124.8, 124.9, 125.4, 125.8, 126.0, 128.4, 128.8, 129.5, 129.9, 130.1, 131.2, 135.3, 136.2, 142.0, 146.7, 147.8, 149.3, 151.8, 153.5, 160.0, 165.4.
- **Compound 8.** % yield: 80%. ^{1}H NMR (*d*-DMSO), δ ppm: 2.89 (s, 6H), 6.44 (m, 4H), 6.61 (m, 4H), 7.07 (dd, 1H), 7.21 (dd, 2H), 7.56 (q, 2H), 7.84 (dd, 1H), 8.87 (s, 1H). ^{13}C NMR (*d*-DMSO), δ ppm: 66.60, 103.2, 104.3, 111.9, 112.5, 113.0, 113.5, 114.0, 123.0, 123.7, 124.5, 124.8, 125.5, 128.9, 129.1, 129.9, 130.1, 131.0, 134.3, 135.3, 151.6, 152.1, 153.2, 153.7, 159.8. 164.4. m.p. 296.62–298.2 °C.

3.4 Preparation of Hydrazone Dye Solutions for Analysis

For metal-dye binding studies (tables 3–6) and fluorescence measurements (figures 6 and 7), the hydrazone dyes and 1 mmol equivalents of metal salt were dissolved separately in 5 mL of DMSO or EtOH. The metal salt solution and hydrazone dye solutions were combined, and the solutions were then illuminated using a bench-top UV lamp ($\lambda_{excitation}$ ~ 365 nm). The lamp was used to survey the solutions for fluorescence. The metal salts used in this study were aluminum (III) nitrate nonahydrate, chromium (III) nitrate nonahydrate, iron (II) perchlorate, iron (Fe) (III) nitrate nonahydrate, and zinc (Zn) (II) perchlorate hexahydrate. The dye-metal binding results are located in tables 3–6. Solutions used in UV measurements were obtained by diluting 1 mL of metal salt-hydrazone dye solutions with 60 mL of EtOH (figures 2–4). UV/Vis experiments were performed using wavelengths of 200–800 nm. The solutions created in the dye-metal binding studies were used directly for fluorescence measurements (figure 5). Emission fluorescence measurements were done with an excitation wavelength of 510 nm.

Table 3. Binding study of hydrazone dyes 6 and 3.

Metals	**Hydrazone Dyes**	
	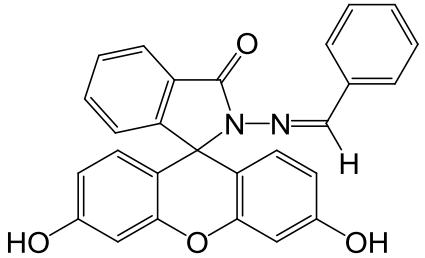	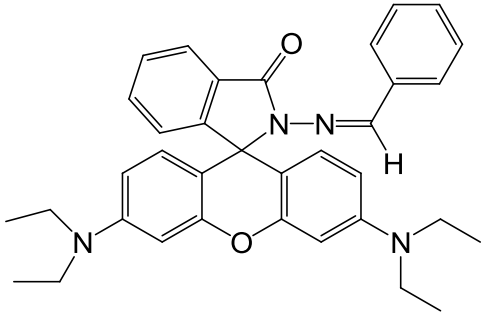
Fluorescence in DMSO		
Blank Fluorescence	No	Yes
Fe^{3+}	No	Yes
Fe^{2+}	No	Yes
Cr^{3+}	No	Yes
Zn^{2+}	No	Yes
Al^{3+}	Insoluble	Insoluble
Fluorescence in EtOH		
Blank Fluorescence	No	Insoluble
Fe^{3+}	No	Yes
Fe^{2+}	No	Yes
Cr^{3+}	No	Yes
Zn^{2+}	No	Yes
Al^{3+}	No	Yes

Table 4. Binding study of hydrazone dyes 5 and 1.

Metals	**Hydrazone Dyes**	
	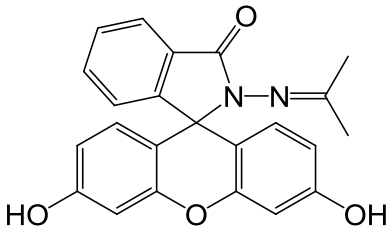	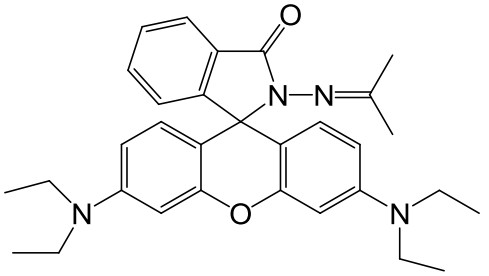
	Fluorescence in DMSO	
Blank Fluorescence	Yes	Yes
Fe^{3+}	**No**	Yes
Fe^{2+}	Yes	Yes
Cr^{3+}	Yes	Yes
Zn^{2+}	Yes	Yes
Al^{3+}	Insoluble	Insoluble
	Fluorescence in EtOH	
Blank Fluorescence	Yes	Insoluble
Fe^{3+}	**Yes**	Yes
Fe^{2+}	Yes	Yes
Cr^{3+}	Yes	Yes
Zn^{2+}	Yes	Yes
Al^{3+}	Yes	Yes

Table 5. Binding study of hydrazone dyes 7 and 4.

Metals	**Hydrazone Dyes**	
	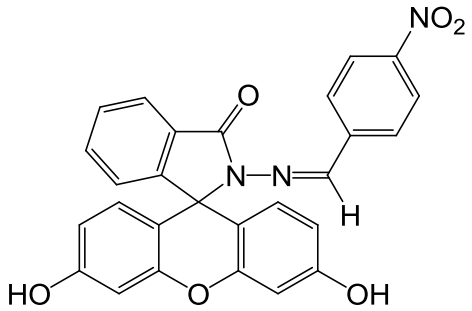	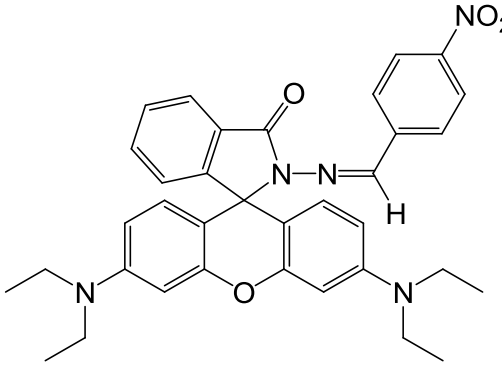
Fluorescence in DMSO		
Blank Fluorescence	No	No
Fe^{3+}	No	No
Fe^{2+}	No	No
Cr^{3+}	No	No
Zn^{2+}	No	No
Al^{3+}	Insoluble	Insoluble
Fluorescence in EtOH		
Blank Fluorescence	No	Insoluble
Fe^{3+}	No	Yes
Fe^{2+}	No	Yes
Cr^{3+}	No	Yes
Zn^{2+}	No	Yes
Al^{3+}	No	Yes

Table 6. Binding study of hydrazone dyes 8 and 2.

Metals	**Hydrazone Dyes**	
	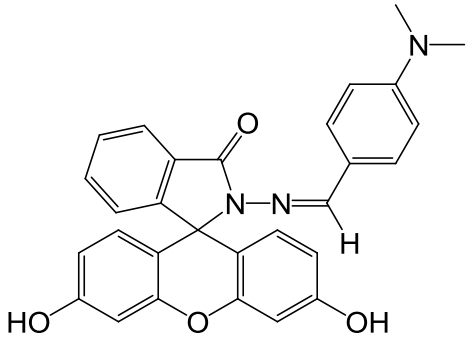	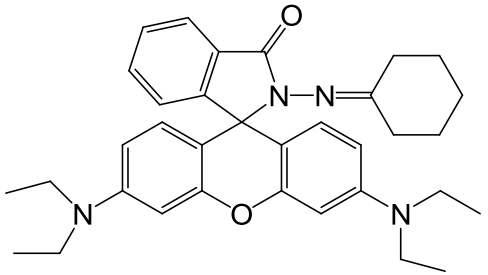
	Fluorescence in DMSO	
Blank Fluorescence	Yes	Yes
Fe^{3+}	Yes	Yes
Fe^{2+}	Yes	Yes
Cr^{3+}	Yes	Yes
Zn^{2+}	Yes	Yes
Al^{3+}	Insoluble	Insoluble
	Fluorescence in EtOH	
Blank Fluorescence	Yes	Yes
Fe^{3+}	Yes	Yes
Fe^{2+}	Yes	Yes
Cr^{3+}	Yes	Yes
Zn^{2+}	Yes	Yes
Al^{3+}	Yes	Yes

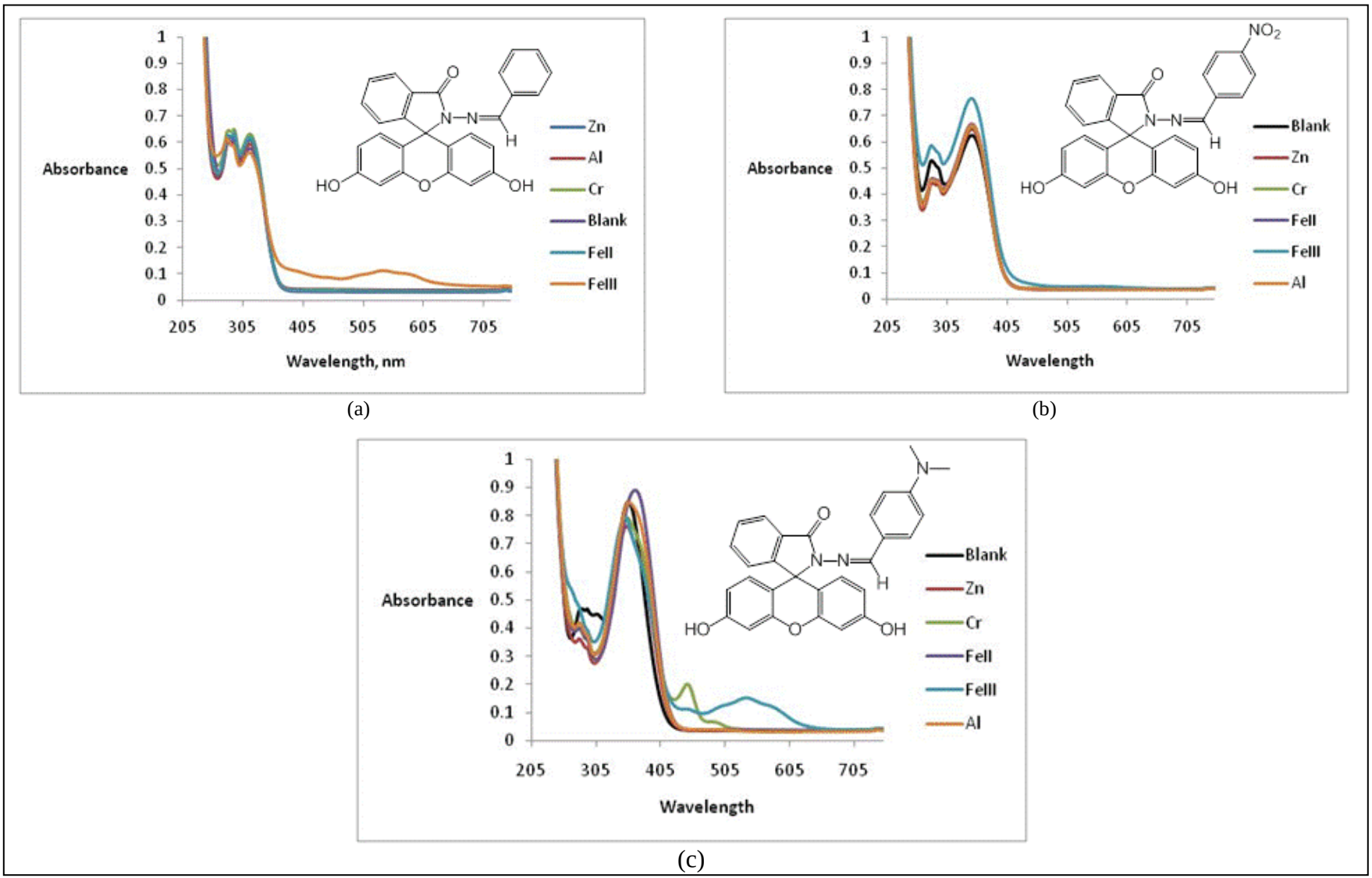

Figure 5. UV and visible absorbance of dye (a) 6, (b) 7, and (c) 8 and metal salts.

4. Discussion

The metal-dye binding results were greatly affected by the solvent system, which influenced solubility, binding, and fluorescence. DMSO dissolved all of the hydrazone dyes and most of the metal salts, except for aluminum (III) nitrate nonahydrate. All metal salts were soluble in EtOH but three of the hydrazone dyes (1, 3, and 4) were insoluble in EtOH. Although some dyes were insoluble in EtOH, once mixed with the metal salt, the dyes dissolved upon complexation with metals.

In some cases, the solvent system also affected fluorescence when comparing dye activity in DMSO versus EtOH (table 5). For example, the nitro substituted rhodamine hydrazone (dye 4) did not fluoresce in DMSO; however, fluorescence was observed in EtOH (figure 6). In another case, 5 did not fluoresce in the presence of Fe^{3+} in DMSO but fluoresced in EtOH (table 4). One explanation could be that DMSO preferentially coordinated with the salts and prevented dye-metal binding.

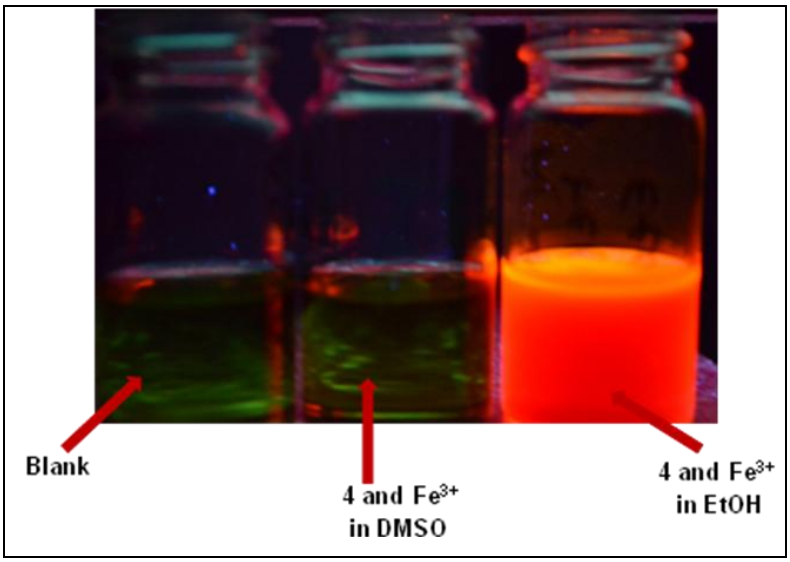

Figure 6. Solvent effect on dye-metal binding and fluorescence observed under UV light.

The dye-metal binding study allowed an assessment of steric and substituent effects, and a direct comparison of fluorescein and rhodamine B dyes with similar structures. Electronic effects were investigated by comparison of dyes with unsubstituted benzene rings and benzene rings with nitro and amino substituents. Steric effects were investigated by comparison of dyes with methyl and cyclohexyl rings. Fluorescein and rhodamine analogs were compared to determine which dye offered the best dye-Fe^{3+} binding selectivity.

The electronics of the substituents greatly affected the dye-metal binding and fluorescence in fluorescein hydrazone dyes. The fluorescein dyes with unsubstituted benzene ring (*6*) and electron withdrawing nitro substituted benzene ring (*7*) did not bind to any metal; however, the dye with the electron donating amino substituted benzene ring (*8*) was fluorescent and bound to all metal salts. No electronic effects were observed in the rhodamine B series as both dye with unsubstituted and nitro substituted benzene rings both bound and fluoresced with all metal salts.

Steric effects were compared between three hydrazone dyes (1, 2, and 5). All dyes bound to all metal salts and fluoresced. In order to get a better understanding of steric effects, a larger set of dyes was needed for comparison.

Based on the dye-metal binding studies, rhodamine based dyes bound to a much larger number of metal salts. However, as the data related to 8 suggested, the presence of electron donating benzene substituents could enhance the dye-metal binding and fluorescence of fluorescein dyes.

Due to fluorescence of unbound rhodamine and fluorescein dyes, UV/Vis and fluorometry measurements were used to identify preferential binding between dyes and individual metal salts. UV analysis showed the role of electronics on dye-metal binding and fluorescence (figure 5). The amino substituent (figure 5c) caused a larger increase in absorbance than the nitro substituent (figure 5b), relative to the dye with an unsubstituted benzene ring (figure 5a). The amino and nitro substituents led to a peak shift (figures 5b and c 370 nm) relative to the unsubstituted ring (figure 5a, 310 nm). The unsubstituted and amino substituted rings (figures 5a and c) had weak absorbances for Fe (III) at 525 nm that were not present for the nitro substituted analog (figure 5b).

Fluorometry experiments showed that sterics caused a change in fluorescence intensity and binding affinity (figures 7 and 8). These measurements investigated the difference in emission fluorescence between FDI (1) and the more sterically hindered 2. For 1 (figure 8), the Fe (II) complex resulted in the highest florescence intensity, closely followed by the zinc (II) complex. Conversely, for 2 (figure 7), the Zn (II) complex had the largest florescence, followed by Fe (II) complex. The Fe (II)-dye 2 complex (figure 7) also had a much lower intensity relative to the Fe (II)-dye 1 (figure 7).

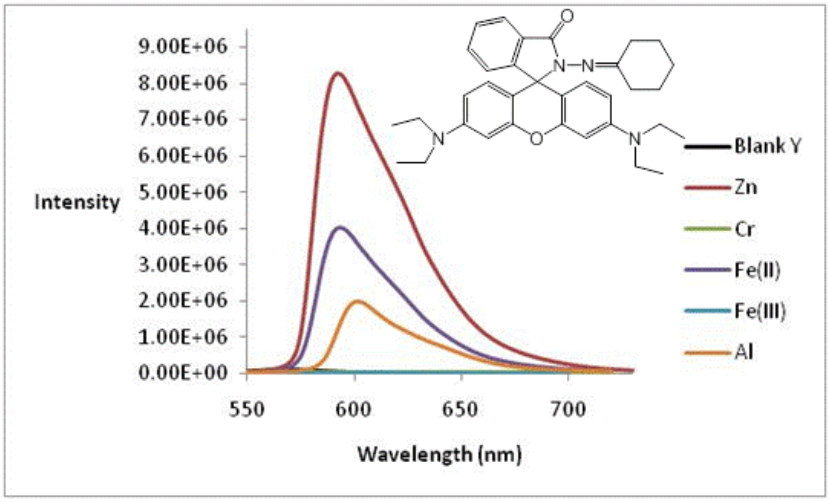

Figure 7. Fluorometry emission intensity measurement of dye 2 and metal salts. Excitation at 510 nm.

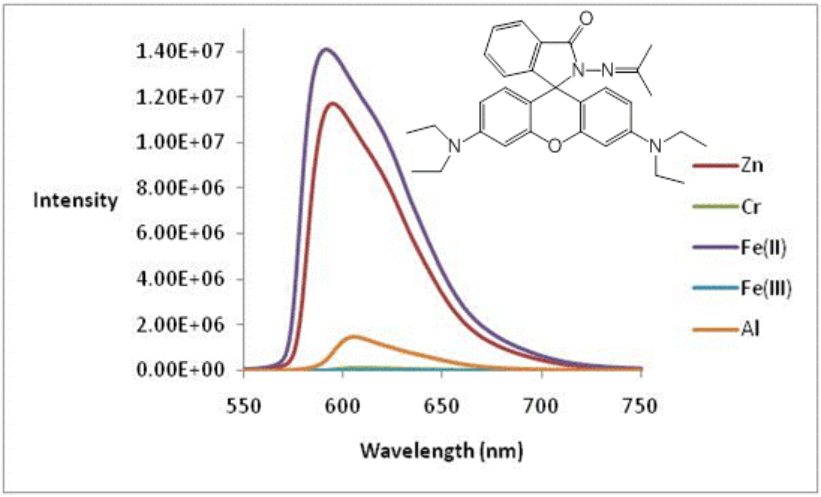

Figure 8. Fluorometry emission intensity measurement of dye 1 and metal salts. Excitation at 510 nm.

5. Future Work

Although the results demonstrated that both steric and electronics affect dye-metal binding and fluorescence, the desired dye-Fe^{3+} binding selectivity was not observed. Therefore, it is important to continue to synthesize additional dyes to further investigate the effects of electronics and steric on dye-metal binding and fluorescence. Dyes will be incorporated into both epoxy (primer) and urethane (topcoat) films to determine the impact of solid state on fluorescence behavior.

6. References

1. Herzberg, E.; Bissell, K.; Crissman, K.; Dovich, J.; Hesson, J.; Kaleba, F.; Mallare, E.; O'Meara, N.; Stevens, B.; Turner, E. *The Annual Cost of Corrosion for the Department of Defense Facilities and Infrastructure*, May 2007.
2. Augustyniak, A.; Tsavalas, J.; Ming, W. *Applied Materials & Interfaces* **2009**, *1*, 2618–23.
3. Hyman, L.; Stephenson, C.; Dickens, M.; Shimizu, K.; Franz, K. *Dalton Transactions* **2010**, *39*, 568–576.
4. Weerasinghe, A.; Schmiesing, C.; Sinn, E. *Tetrahedron Letters* **2009**, *50*, 6407–6410.
5. Wu, J.-S.; Kim, H. J.; Lee, M. H.; Yoon, J. H.; Lee, J. H.; Kim, J. S. *Tetrahedron Letters* **2007**, *48*, 3159–3162.
6. Xiang, Y.; Tong, A.; Peiyuan, J.; Ju, Y. *Organic. Letters* **2006**, *8*, 2863–2866.
7. Yang, H.; Zhou, Z.; Huang, K.; Yu, M.; Li, F.; Yi, T.; Huang, C. *Organic Letters* **2007**, *9*, 4729–4732.
8. Zhang, X.; Shiraishi, Y.; Hirai, T. *Organic Letters* **2007**, *9*, 5039–5042.
9. Zhang, M.; Gao, Y.; Li, M.; Yu, M.; Li, F.; Li, L.; Zhu, M.; Zhang, J.; Yia, T.; Huang, C. *Tetrahedron Letters* **2007**, 483709–3712.

7. Transitions

The following oral presentations have been prepared:

- Williams, A. A.; Orlicki, J. A.; Escarsega, J. A.; Labukas, J.; Placzankis, B. Effects of sterics and electronics on metal binding of fluorescent molecules: Towards smart coating materials, 242nd ACS National Meeting & Exposition, Denver, CO, August 28–September 1, 2011.
- Williams, A. A.; Labukas, J.; Orlicki, J. A.; Escarsega, J. A.; Placzankis, B. Synthesis and Application of Rhodamine B and Fluorescein Corrosion Sensing Dyes, 243rd ACS National Meeting & Exposition, San Diego, CA, March 2012. Abstract submitted.

List of Symbols, Abbreviations, and Acronyms

Al	aluminum
$CDCl_3$	deuterated chloroform
Cu	copper
Cr	chromium
DMSO	dimethylsulfoxide
DoD	Department of Defense
EtOH	ethanol
FDI	spiro[1H-isoindole-1,9'-[9H]xanthen]-3(2H)-one, 3',6'-bis(diethylamino)-2-[(1-methylethylidene)amino]
Fe	iron
HCl	hydrochloric acid
Hg	mercury
MeOH	methanol
NaOH	sodium hydroxide
NMR	nuclear magnetic resonance
Pb	lead
rt	room temperature
UV	ultraviolet
Vis	visible
Zn	zinc

NO. OF COPIES	ORGANIZATION
1 ELEC	ADMNSTR DEFNS TECHL INFO CTR ATTN DTIC OCP 8725 JOHN J KINGMAN RD STE 0944 FT BELVOIR VA 22060-6218
1	US ARMY RSRCH LAB ATTN RDRL WMM C B E PLACZANKIS ABERDEEN PROVING GROUND MD 21005
1	US ARMY RSRCH LAB ATTN RDRL WMM G J ORLICKI BLDG 4600 ABERDEEN PROVING GROUND MD 21005
3	US ARMY RSRCH LAB ATTN RDRL WML D A W WILLIAMS ATTN RDRL WMM C J ESCARSEGA ATTN RDRL WMM C J LABUKAS ABERDEEN PROVING GROUND MD 21005-5066
3	US ARMY RSRCH LAB ATTN IMNE ALC HRR MAIL & RECORDS MGMT ATTN RDRL CIO LL TECHL LIB ATTN RDRL CIO LT TECHL PUB ADELPHI MD 20783-1197